

Lawrence Berkeley National Laboratory

Lawrence Berkeley National Laboratory

Title

CO prompt emission as a CO₂ marker in comets and planetary atmospheres

Permalink

<https://escholarship.org/uc/item/27b6k576>

Author

Kalogerakis, Konstantinos S.

Publication Date

2013-05-20

1 *CO prompt emission as a CO₂ marker in comets and planetary atmospheres*

2 Konstantinos S. Kalogerakis,^{a*} Constantin Romanescu,^{a,b} Musahid Ahmed,^c Kevin R.

3 Wilson,^c and Tom G. Slanger,^a

4 ^a Molecular Physics Laboratory, SRI International, Menlo Park, CA 94025 USA

5 ^b Present address: Department of Chemistry, Brown University, Providence, RI 02912,
6 USA

7 ^c Chemical Sciences Division, Lawrence Berkeley National Laboratory, Berkeley, CA
8 94720 USA

9 * Corresponding author. Email: ksk@sri.com, FAX: (650) 859-2111

10

11 Pages: 21

12 Figures: 5

13 Tables: 0

14

15

16 **Proposed Running Head:** CO prompt emission in comets and planetary atmospheres

17

18

19 **Abstract**

20 Observations of CO emissions in the visible and near-infrared (NIR) have been rare for
21 comets, and no measurements from orbiters are currently available in the visible for the
22 dayglows of Mars or Venus. Analysis of the ultraviolet CO(*a-X*) Cameron bands from
23 Mars Express dayglow observations supports the conclusion that these bands have very
24 high rotational temperatures, some thousands of kelvins. The most plausible source for
25 the CO rotational excitation is its generation by CO₂ photodissociation. Recent laboratory
26 measurements investigating the photodissociation of CO₂ in the extreme ultraviolet
27 (EUV) reveal strong emissions in the visible and NIR region by the triplet CO(*a'*, *d*, *e*)
28 states, which we take to be a primary source for the UV CO(*a-X*) Cameron bands. Thus,
29 detection of visible emissions from the triplet CO states in planetary dayglows and
30 comets provides an upper limit to the CO₂ density. The presence of CO high rotational
31 excitation along with the intense visible and NIR band emissions should be considered as
32 a practical way by which planetary dayglow and cometary spectra provide information on
33 the presence of CO₂. Finally, we report on existing observations of cometary atmospheres
34 and estimate the altitude for the emitting layer of the CO triplet states in Mars and Venus.

35 *Icarus* Keywords: Mars atmosphere, Venus atmosphere, spectroscopy, photochemistry,
36 Comets

37

38

39 **Introduction**

40 CO₂ is the dominant species in the atmospheres of Mars and Venus. It can also be
41 a significant component in comets and in the atmospheres of extrasolar planets.

42 Therefore, the details of CO₂ photochemistry are critical in interpreting the airglows of
43 these bodies. A great deal is known from relevant laboratory investigations, but several
44 issues have not yet been addressed by atmospheric observations, either in ground-based
45 studies or those from orbiters.

46 A major problem is that space observations are typically designed to view UV and
47 IR emissions to the exclusion of visible spectra. In principle, part of the reason for this is
48 that the visible spectral region can be investigated from ground-based studies, which are
49 not blocked by ozone in the UV and by water and other components in the IR. However,
50 this is an inadequate rationale, because only the Venus nightglow can be studied from the
51 ground. Dayglows require orbital observations, as is also true for the Mars nightglow.
52 Because Mars' orbit is exterior to that of Earth, its nightglow is practically inaccessible
53 from the ground.

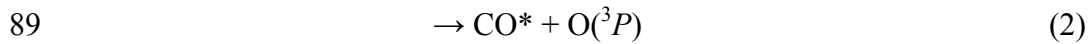
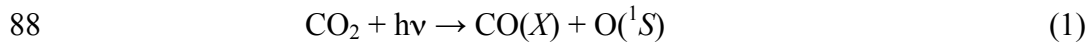
54 There are common emissions in the terrestrial atmosphere that must have their
55 counterparts on Venus and Mars but have not yet been observed from orbit. Foremost
56 among these are the green and red lines of the oxygen atom, at 557.7 nm and
57 630.0/636.4 nm, to which we can also add the 777.4 and 844.6-nm lines. In the case of
58 the O(¹S-¹D) green line, there is the O(¹S-³P) surrogate at 297.2 nm, which has an
59 intrinsic intensity that is weaker by a factor of 9.5 [*Slanger et al.*, 2006a, 2011a;
60 *Gattinger et al.*, 2009, 2010]. This UV emission is well known in the Mars dayglow from
61 information gained in both the Mariner and Mars Express missions.

62 The green line has been studied from the ground in the Venus nightglow [*Slanger*
63 *et al.*, 2001, 2006b, 2011a], and it was a somewhat surprising addition to the Venus
64 features because it did not appear in the Venera visible spectra [*Krasnopolsky et al.*,
65 1976, 1983], which was the only previous visible nightglow measurements of Venus.
66 These early experiments have now been duplicated by Venus Express [*Garcia-Muñoz et*
67 *al.*, 2009], still without the appearance of the green line. Based on several observations
68 from the ground, the green line emission appears to be highly variable [*Slanger et al.*,
69 2006b, 2011b]. Slanger and Fox [2009] have recently proposed an ionospheric source for
70 $O(^1S)$ that follows the solar cycle, accounting for the current lack of detection.

71 CO_2 photodissociation, in addition to giving excited atomic oxygen states,
72 generates excited states of CO. The $CO(a-X)$ Cameron band emission, in the range
73 180-260 nm, has been known ever since the Mariner days. Lawrence [1972a] investigated
74 the production of the Cameron bands from CO_2 photodissociation below 108 nm and
75 characterized the yield as a function of the photon energy. However, at energies greater
76 than 12.4 eV (photon wavelength less than 100 nm), other channels open up, and the
77 ultimate source of the Cameron bands becomes complicated.

78 In the 11-14 eV region, photoabsorption by CO_2 is strong and very structured
79 [*Chan et al.* 1993]. Photoionization starts at 13.8 eV, accounting for a rapid decrease in
80 the absorption cross-section. Other important emissions in the UV Mars dayglow include
81 the $CO_2^+(B-X)$ 0-0 band at 289 nm and the $CO_2^+(A-X)$ bands above 300 nm, which
82 require 18.1 eV and 17.3 eV, respectively, for direct excitation. It has been suggested
83 [*Leblanc et al.*, 2006] that at least part of the $CO_2^+(B)$ excitation comes from
84 photoexcitation of $CO_2^+(X)$.

85 Production of the CO excited states begins near 11.5 eV, which corresponds to the
86 threshold for CO(*a*) formation [Lawrence, 1972a]. The 10.5-13.8 eV region is dominated
87 by two types of dissociation,



90 where CO* corresponds to the four triplet levels—*a*³*Π*, *a*'³*Σ*⁺, *d*³*Δ*, *e*³*Σ*⁻. Emission
91 from the *a*' , *d*, and *e* states down to *a*³*Π* are known as the Asundi, Triplet, and Herman
92 bands, respectively, and have associated radiative lifetimes of a few microseconds. Thus,
93 *a*'-*a*, *d*-*a*, and *e*-*a* emissions are prompt in planetary and cometary atmospheres. The
94 radiative lifetime associated with the *a*-*X* Cameron bands is about three orders of
95 magnitude longer than for the triplet bands. Thus the Cameron band intensity is sensitive
96 to the altitude in planetary dayglow, which will not be true for the triplet bands. Both
97 emissions are prompt in comets.

98 The O(¹*S*) yields from CO₂ photodissociation have been determined [Lawrence,
99 1972b], and the sum of the CO* and O(¹*S*) yields over the stated energy region is not far
100 from unity, although for the O(¹*S*) case, Lawrence suggests that the accuracy may not be
101 better than a factor of two. It is important to note that the instrumental resolution with
102 which the measurements were made was much coarser than the structure in the CO₂
103 absorption spectrum. However, for the Cameron bands, Lawrence showed that there was
104 no correlation between the spectral structure and the apparent yield—the latter was a
105 smooth function of the wavelength alone, rising from zero at the threshold at 108 nm to
106 50–60% at 90 nm. The measurements for O(¹*S*) were much less extensive because of the
107 weakness of the signal, but the absence of a yield dependence on the cross section for

108 CO(*a*) (including the higher triplet states) carries the implication that the same is true for
109 O(¹*S*). The production of O(¹*S*) occurs in a low cross-section region, while the CO triplet
110 bands are generated in a region of shorter wavelength and large cross section.

111 If we consider the product of the CO₂ absorption cross section and the solar flux,
112 we can demonstrate that the most important region for solar photodissociation is at
113 90-110 nm [*Huestis et al.*, 2008], just the region where the CO(*a*) yield is highest
114 [*Lawrence*, 1972a]. Noteworthy is the fact that the very strong Lyman-alpha (Ly-α) line
115 at 121.6 nm is much less important than the shorter wavelength radiation.

116 Interest in CO₂ photodissociation in the solar system is not limited to the
117 atmospheres of Mars and Venus. Cometary atmospheres contain substantial amounts of
118 CO₂, and what we learn about the dayglows of Mars and Venus has direct application to
119 cometary spectra—the photon source being, in both cases, the sun. Thus, comparisons
120 among Mars spectroscopic results, those from comets, and those from relevant laboratory
121 studies can help improve our understanding of these systems. Finally, we would expect
122 similar principles to be applicable to CO₂ planetary atmospheres in other solar systems.

123

124 **Evidence from Observations and Laboratory Experiments**

125 *Highly Rotationally Excited CO in the Mars Dayglow*

126 UV spectra of Mars dayglow were initially obtained by the Mariner spacecraft
127 [*Barth et al.*, 1971], and more recently by the Spectroscopic Investigation of the
128 Characteristics of the Atmosphere of Mars (SPICAM) spectrometer on Mars Express
129 [*Leblanc et al.* 2006]. SPICAM has a long wavelength cut-off near 310 nm, while the
130 Mariner instruments made measurements to 400 nm.

131 An example of the SPICAM spectra is shown in Figure 1, where the three most
132 important dayglow emissions are seen—the CO Cameron bands, the $\text{CO}_2^+(B-X)$ 0-0 band,
133 and the $\text{O}(^1S-^3P)$ line. The Ly- α geocoronal line is a strong feature at shorter
134 wavelengths. For both Mars and Venus, solar scattering from haze and clouds can affect
135 the spectra, but for Mars it is not an issue for tangent ray heights greater than 130 km and
136 for lower altitudes corrections can be made. For the Spectroscopy for Investigation of
137 Characteristics of the Atmosphere of Venus (SPICAV) spectrometer on Venus Express,
138 the problem is much more severe, and there are as yet no published data, although it is
139 reasonable to expect that the same features will appear.

140 It was pointed out long ago [Conway, 1981] that the Mariner Cameron band
141 spectra showed a very hot rotational distribution. The analysis gave a bimodal
142 temperature, the best fit showing both 1600 K and 10,000 K. This is an extraordinary
143 result and, in our recent analysis of results from the Mars Express SPICAM instrument,
144 we found such a distribution.

145 Figure 2 shows a series of DIATOM™ [Huestis, 1994] simulations of the intensity
146 distribution of the Cameron bands in the Mars dayglow. They are composed of the $v' =$
147 0–2 band sequences, using published Franck-Condon factors [Krupenie, 1966], with
148 slight adjustments to improve the relative amplitudes. The calculations are carried out for
149 single temperatures from 500 K to 10,000 K. The thick solid line is a representative
150 SPICAM spectrum; overall, it falls between the 4000 and 6000 K lines. Thus, we concur
151 with Conway's analysis, in which he also investigated whether the $\text{CO}^+(B-X)$ First
152 Negative bands might be present in this region, thus filling in the intensity between the
153 Cameron bands. He concluded this system was not present. The resolution of the

154 SPICAM instrument is demonstrated by the appearance of the 297.2 nm atomic line,
155 which shows that the bands are much wider.

156 As noted, there are no Mars/Venus visible dayglow spectra against which to
157 check for the presence of the three CO triplet sequences, but there are visible ground-
158 based cometary spectra, and we can look for evidence of both hot CO(*a*) distributions and
159 the triplet bands.

160

161 *Laboratory Studies of CO Emission Following CO₂ Photodissociation*

162 From laboratory experimental work, it becomes clear that the CO triplet systems
163 can be useful ground-based markers for CO₂ in cometary atmospheres, so any high-
164 resolution cometary study should include a search for these features. These states can be
165 generated by direct excitation of CO by photons or electrons, although the $X \rightarrow a'$, d , e
166 transitions are spin-forbidden. Thus, appearance of the visible bands cannot be taken as
167 conclusive proof of the presence of CO₂. Their absence, however, should be interpreted
168 as an indication that little or no CO₂ and CO are present.

169 Although CO Cameron band emission is the best-known product of CO₂
170 photodissociation in planetary atmospheres, these higher CO states can cascade into
171 CO(*a*), the emitting Cameron band state. There is a limited early history on this topic
172 [*Judge and Lee, 1973; Lee and Judge, 1973*], and it is clear that with increasing photon
173 energy, these states become important. CO(*a*) is first produced at 11.46 eV, and the three
174 higher-lying triplet levels that are nearby, a' , d , and e , have thresholds at 12.31, 12.97,
175 and 13.35 eV, respectively. The optical transitions from these levels to the CO(*a*) state
176 are fully allowed, and any population excited to these higher levels cascades to CO(*a*),

177 because the transition to the ground-state is not optically allowed, except for localized
178 perturbations [Tilford and Simmons, 1972; Slanger and Black, 1970]. These cascading
179 pathways generate both visible and NIR emission, and provide a diagnostic for the
180 presence of CO₂.

181 Laboratory studies of the CO excited states have been carried out for a variety of
182 reasons—for pure spectroscopy, for combustion chemistry, and to understand planetary
183 atmospheres. In combustion research, Burke *et al.* [1996] discovered that both the CO
184 Cameron bands and the visible triplet bands were formed from two separate reactions—
185 that of oxygen atoms with acetylene and with the C₂O molecule. Normally, this should
186 have little relevance to cometary and planetary issues but, in fact, the emission patterns in
187 both the UV and the visible are indiscernible from what we recently observed in relevant
188 laboratory studies on the EUV photodissociation of CO₂ (C. Romanescu, K.S.
189 Kalogerakis, T.G. Slanger, L.C. Lee, M. Ahmed, and K. R. Wilson, manuscript in
190 preparation, 2012) and, for the UV, from what was seen at Mars by the Mariner
191 spacecrafts [Barth *et al.*, 1971] and by Mars Express [Leblanc *et al.*, 2006]. It is not clear
192 why this should be so, but we can make use of the information to learn about the NIR
193 region, where neither the planetary probes nor the laboratory experiments have provided
194 results yet. In the work of Burke *et al.* [1996], the most intense band is the *a'-a* 2-0 band,
195 at 1.08 μ, which ought to be a target for cometary and planetary dayglow observations.
196 We have looked for this emission in a published spectrum of Comet West [Johnson *et al.*,
197 1983], and its absence may indicate that the coma contains very little CO₂.

198 To observe the visible CO triplet bands, the energetics require that we carry out
199 CO₂ photodissociation measurements in the 11-14 eV range. Details of the experimental

200 apparatus and results are described elsewhere (*Romanescu, et al.*, manuscript in
201 preparation, 2012), and only a brief account is reported here. As the required light source
202 must operate in the “windowless” spectral region, we ran the measurements in a reaction
203 cell that was coupled to the direct output of the undulator at the Chemical Dynamics
204 Beamline (9.0.2) at the Advanced Light Source of the Lawrence Berkeley Laboratory
205 (ALS). Because of the large pressure differential—some twelve orders of magnitude
206 between the ring and the reaction cell—it was necessary to build a series of differential
207 pumping sections, so that the pressure in the reaction cell region could be made
208 compatible with the ring pressure of 10^{-10} Torr. The beam flux entering the cell is
209 nominally 10^{16} photons per second per 2.5% bandwidth, or 4×10^{15} photons per second
210 per nm at a wavelength of 100 nm. The gas samples consisted of either 0.1% CO₂ in He
211 (Matheson, Certified mixture grade) or pure CO₂ (Matheson, 99.995%).

212 Two principal types of measurements were carried out: excitation spectra and
213 fluorescence spectra. In an excitation spectrum, we choose a detection wavelength and
214 pressure, and scan the photon energy, to determine how the signal intensity behaves. This
215 is determined by a combination of photoabsorption cross sections, photon flux, and
216 fluorescence yields, all as a function of wavelength. The visible and UV emissions from
217 the cell were measured simultaneously with filtered photomultiplier tubes (PMT). For the
218 Cameron bands, we used a 10-nm full-width half-maximum (FWHM) interference filter
219 centered at 214 nm, i.e., the position of the CO(*a-X*) 0-1 band. For the visible emission,
220 we employed a 520-nm long-pass filter, so that all emission was collected out to the
221 photomultiplier tube (PMT) cut-off (~850 nm), although much of the emission is from
222 longer wavelengths. In Figure 3, we show two excitation spectra for a mixture containing

223 ~4 mTorr CO₂ in 2 Torr He, one for the Cameron bands, and the other for emission in the
224 520 to 850-nm range. The intensities are normalized to the peak.

225 The spectra show different behavior, because the threshold for direct Cameron
226 band production is ~1 eV lower than the triplet band threshold. Furthermore, the various
227 triplet bands will not be registered at their threshold, because the emission will first
228 appear in the IR, where our detector is not sensitive. With increasing photon energy, the
229 emission moves into the visible and is recorded. From Figure 3, we can see that the
230 Cameron band signal becomes large in line with the visible signal, indicating that the
231 cascading contributions are a major Cameron band source.

232 After having determined that the maximum signal at both wavelength regions is at
233 a photon energy of 13.4 eV (92.5 nm), we recorded fluorescence spectra using a
234 monochromator and photon counting arrangement. The spectra were calibrated utilizing
235 the phototube sensitivity and the monochromator grating efficiency, both to set the
236 photon fluxes on a comparable scale with respect to the two spectral regions, and to carry
237 out an extension into the IR. Because the phototube is not sensitive in the IR region,
238 where much of the triplet emission is found, we can use the calibrated IR spectrum
239 [Burke *et al.*, 1996] to extend the spectrum. In this manner, we can evaluate how much of
240 the light is missing from the UV and visible region. By using the 785-nm *a'-a 5-0* band—
241 common to both spectra—it is possible to make this comparison.

242 Figure 4 shows the complete calibrated spectrum, from the UV to the IR,
243 corrected for phototube sensitivity and grating efficiency, and extended into the IR by
244 digitizing and adding the Burke *et al.* [1996] spectrum beyond 785 nm. The bands are
245 tabulated elsewhere (*Romanescu, et al.*, manuscript in preparation, 2012), and higher

246 resolution data would be helpful in clarifying ambiguities. It is intriguing that the UV
247 portion of the spectrum of Figure 4 has most of the features of the Mars dayglow, which
248 further supports the notion that the visible/IR portion reproduces the as-yet-unobserved
249 dayglow spectrum in that region.

250 The spectrum of Figure 4 and its extension into the IR to 1.4 μm shows that there
251 is much more visible/IR emission than Cameron band emission for the excitation energy
252 of 13.4 eV. For the studied mixture of ~ 6 mTorr CO_2 in 4 Torr He, the integrated
253 [triplet]/[Cameron] intensity ratio is approximately 9. This factor depends on the CO_2
254 density. With decreasing density, the Cameron bands become larger relative to the $a'-a$
255 and $d-a$ bands, as the $\text{CO}(a)$ radiating efficiency increases. We can thus conclude that the
256 visible/IR CO triplet bands must be a major emission feature in the Mars/Venus
257 dayglows, where there is no question of the importance of CO_2 photoabsorption. In
258 comets, the triplet bands will be significant if CO_2 is an important atmospheric
259 component.

260 If the triplet bands were produced exclusively at 13.4 eV, and then cascaded to the
261 $a^3\Pi$ state, the production rates in the two regions would be equal. However, the UV and
262 visible/IR *intensities* will not be equal, because the Cameron bands are quenched by CO_2 ,
263 whereas the triplet bands are not. Thus, the fact that the Cameron bands are nine times
264 weaker than the triplet bands in Figure 4 is an indication of this effect. The single $a'-a$
265 Asundi 2-0 band at 1.08 μ is twice as intense as the entire Cameron band system.

266 With regard to laboratory observations in condensed media, Gudipati and Kalb
267 [1998] have carried out experiments in which CO/Ar mixtures were irradiated near
268 155 nm, while Wagner et al. [2000] did the same in CO_2 /Ar mixtures. In both cases the

269 visible/near IR CO triplet transitions were observed, preceding the Cameron bands. In
270 the study on CO₂, CO was initially produced, which was then excited. Interesting to note
271 is that in the CO study the strongest triplet feature is the *a'-a* 2-0 band, just as seen in
272 Figure 4.

273

274 *CO Emissions in Cometary Spectra*

275 We now examine previously reported observations of cometary spectra in light of
276 the information presented above. Since CO₂ in the cometary and planetary environments
277 will interact similarly with solar radiation, we expect to see a hot distribution in the case
278 of comets if CO₂ is a significant component. Weaver et al. [1994] and Feldman et al.
279 [1997] have studied this and, although the Cameron bands could be detected in the
280 observed comets, there was little indication of the hot distribution reported by Conway
281 [1981]. On this basis, they concluded that the Cameron bands were not formed from CO₂
282 photodissociation, but more likely were the product of direct photoelectron excitation of
283 CO. These observations provide further evidence that CO₂ is not a major component in
284 most cometary atmospheres and, in fact, it is generally accepted that the [CO₂]/[H₂O]
285 ratio is 0.05-0.1, based on IR absorption measurements [M. A Hearn, private
286 communication, 2008].

287 In addition to the UV Cameron bands, there are a number of claims to
288 observations of the three CO triplet sequences in comets. Discussions of the presence of
289 these systems rarely go beyond noting their identification, and much of this identification
290 is suspect. There are several papers by the group of K.I. Churyumov [1997, 2003]
291 claiming identifications of the Asundi and Triplet systems in comet C/1989 Y1

292 Skorichenko-George. They are far from convincing. Not only are bandhead positions up
293 to 0.5 nm away from “theoretical” positions, but the latter are merely rather inaccurate
294 laboratory measurements from earlier times. Additionally, the spectra shown in these
295 papers do not convey to the viewers that the bands are real. A recent article by Picazzio et
296 al. [2007] presents data that suffer from the same problems.

297 The most convincing identification of the triplet bands comes from spectra of
298 Comet Bradfield [*Cosmovici et al.*, 1982]. There are several candidates between 630 and
299 740 nm, in the region of strong Asundi and Triplet bands. However, at longer
300 wavelengths, where the Asundi/Triplet bands in our spectra get stronger, there are no
301 clear identifications in the cometary spectrum.

302 Cochran and Cochran [2002] have published an extensive list of emission lines
303 seen in Comet 122P/de Vico—more than 16,000 lines were found, of which 12,000 could
304 be identified. None of these lines were identified as belonging to the CO triplet systems.

305 Overall, positive observations of CO visible emissions from comets are not at all
306 common in the literature, a fact that highlights the relative scarcity of CO₂ in cometary
307 composition.

308

309 *CO Triplet Band Intensity Estimates in Comets*

310 We can combine our laboratory data with models for cometary Cameron band
311 emission to make approximate predictions of the intensity of the CO bands in the visible
312 and near-infrared regions. Raghuram and Bhardwaj [2012] have recently published a
313 model of CO Cameron band emission associated with Comet 1P/Halley. They have
314 made the claim that the Cameron band source is not limited to CO₂ photodissociation, as

315 in earlier models [*Weaver et al.*, 1994; , *Feldman et al.*, 1997], but that photoelectron
316 collisions on CO₂ is actually the more important mechanism. Still, they assign 20-30% of
317 the Cameron band production to the CO₂ + hv process, although they do not invoke
318 cascading from the CO(*a'*, *d*, *e*) levels as a source of CO(*a*).

319 For P1/Halley, the values given for the total slit-averaged brightness for the
320 Cameron bands measured by the International Ultraviolet Explorer (IUE) is of the order
321 of several hundred Rayleighs [*Raghuram and Bhardwaj*, Table 3]. If we take 25% as a
322 value for the fraction of Cameron bands coming from CO₂ photodissociation, then the
323 intensity from this source is on the order of 100 R. As we make the claim that most of
324 the observed Cameron band emission arising from CO₂ photodissociation is preceded by
325 cascading from the CO(*a'*, *d*, *e*) states, then the visible/near-IR emission from these states
326 is predicted to be of this same magnitude, ~100 R, spread over the 600 to >1400 nm
327 range shown in Figure 4. Because of reduced sensitivity of detectors in the IR, probably
328 the best band to view in a search for the triplet emissions is the *a'-a* 5-0 band (the shortest
329 wavelength head of the quintuple-headed band lies at 783 nm [*Krupenie*, 1966]), where
330 an estimated intensity for this band alone is about 10% of the total, i.e. ~10 R.

331 However, the 75% fraction of the Cameron bands that are claimed to arise from
332 photoelectrons on CO₂ [*Raghuram and Bhardwaj*, 2012] do not exclude similar CO
333 products, considering that the energy threshold for CO(*a*) production from CO₂ is
334 11.5 eV, whereas that for CO(*a'*) production is 12.3 eV. Therefore the 10 R estimate for
335 the intensity of the *a'-a* 5-0 band is a lower limit, an upper limit being larger by a factor
336 of four.

337

338

339

340 **Altitude of the CO Triplet Band Emission in Venus and Mars**

341 Although we can conclude that the CO triplet bands are produced with high
342 efficiency in CO₂ photodissociation at energies around 13.4 eV, it is necessary to
343 consider how photons are absorbed in the CO₂ atmospheres, which sets constraints on the
344 observations. The crux of the matter is that 13.4 eV photons are blocked by CO₂ at
345 relatively high altitudes. Above such altitudes, the Cameron and triplet bands will have
346 comparable intensities, but at the altitude where the Cameron band profile peaks,
347 typically near 120 km in the Mars dayglow [*Simon et al.*, 2009], the unity optical depth
348 (1/e absorption) for 13.4 eV photons will be higher. To quantify the photoabsorption
349 process, it is useful to calculate the altitude of unity optical depth. This has been done for
350 the Venus atmosphere [*von Zahn*, 1980], but not at the resolution of the CO₂ absorption
351 cross sections presented in Figure 1. For the calculation, we integrate a CO₂ altitude
352 profile from the top of the atmosphere downwards and use the photoabsorption cross
353 section as a function of wavelength [*Chan et al.*, 1993],

$$354 \quad 1 = \alpha(\lambda) \int N_{\text{CO}_2}(h) dh \quad (3)$$

355 where $\alpha(\lambda)$ is the wavelength-dependent cross section and $N_{\text{CO}_2}(h)$ is the number density
356 as a function of altitude. In Figure 5, the calculation is performed for both the Mars and
357 Venus atmospheres, for a vertical sun, using the profiles given by Fox and Dalgarno
358 [1979] and Fedorova et al. [2009] for Mars, and Krasnopolsky and Parshev [1983] for
359 Venus. We see that for 13.4 eV photoexcitation, unity optical depth is reached at 137 km
360 for Venus and 131 km for Mars. Therefore, for the case of Mars, the CO triplet band

361 emission generated by CO₂ photodissociation for 1/e absorption will lie only 11 km
362 higher than the 120 km Cameron band peak seen by SPICAM [*Simon et al.*, 2009].

363 When cascading from the upper triplet levels is the dominant source of the
364 Cameron bands, most of the emission comes from the $a(v = 0)$ level, because a large
365 fraction of the visible/IR emission terminates on that level. We can estimate a quenching
366 factor for $a(v = 0)$ from its radiative lifetime and the CO₂ removal rate coefficient. The
367 latter has been measured, with a range of $(1.2-1.7) \times 10^{-11} \text{ cm}^3\text{s}^{-1}$ [*Slanger*, 1971; *Taylor*
368 *and Setser*, 1971; *Wysong*, 2000]. The radiative lifetime of the $a^3\Pi$ state is dependent on
369 rotational level; the most recent value for the CO($a^3\Pi_1$, $v = 0$, $J = 1$) level is about 3 ms
370 [*Gilijamse et al.*, 2007]. Thus, the CO₂ density for which the collisional quenching and
371 radiative rates are equal is about $2.2 \times 10^{13} \text{ cm}^{-3}$. For Mars, this corresponds to an altitude
372 of ~80 km, and for Venus, ~120 km. Thus, for the 1/e penetration depths shown in Figure
373 5, quenching is unimportant for the CO(a) state and non-existent for the higher triplet
374 states for photon energies above the CO(a) threshold of 11.45 eV. Emission from higher
375 altitudes should have the signature of approximately equal contributions from the
376 Cameron and visible-IR systems. However, as the altitude decreases, there are competing
377 factors; lower energy photons will lead to increasing production of nascent CO(a) that is
378 unaccompanied by triplet emission, and increasing density will preferentially quench
379 CO(a).

380

381 **Conclusions**

382 CO₂ photodissociation in the extreme UV is of particular interest to our
383 understanding of cometary spectra and of the Mars and Venus dayglows. The UV CO

384 Cameron bands are well-known features of these systems, but there have been essentially
385 no attempts to observe other CO emissions that lie in the visible and NIR spectral
386 regions. Because these emissions can be a source of the Cameron bands *via* cascading, it
387 is important to evaluate their yields.

388 At the peak of the CO₂ absorption region, near 13.4 eV photon energy, the yields
389 of visible/NIR emissions are essentially equal to the Cameron band yields. It follows that
390 most of the Cameron band intensity originates with cascading from higher levels at that
391 photodissociation energy, rather than from direct excitation. The visible/NIR emission is
392 strongest at wavelengths longer than 1.0 μm. Detection of this emission in cometary
393 atmospheres and in the planetary dayglows provides an upper limit to the CO₂ density.
394 The presence of CO high rotational excitation along with the intense visible and NIR
395 band emissions should be considered as a reliable indicator of the presence of CO₂ in
396 planetary and cometary atmospheres. A search for CO triplet band emission in the
397 Mars/Venus dayglows should be conducted at altitudes somewhat above the peaks in the
398 Cameron band emission.

399

400 **Acknowledgements**

401 This work was performed under grant NNX06AB82G from the NASA Outer
402 Planets Research Program to SRI International. Partial support from NSF grants AST-
403 0709173 and AST-1109372 is also acknowledged. We are grateful to W.L. Dimpfl of
404 Aerospace Corp. for providing laboratory spectra from their flow discharge studies, to the
405 staff at ALS for technical support, and to our colleagues D. L. Huestis and L. C. Lee for
406 helpful advice and discussions. M. Ahmed, K.R. Wilson, and the ALS are supported by

407 the Director, Office of Energy Research, Office of Basic Energy Sciences, Chemical
408 Sciences Division of the U.S. Department of Energy under contract No. DE-AC02-
409 05CH11231.

410

411 **References**

412 Barth, C.A., C.W. Hord, J.B. Pearce, K.K. Kelly, G.P. Anderson, and A.I. Stewart, 1971.
413 Mariner 6 and 7 ultraviolet spectrometer experiment: Upper atmosphere data. *J. Geophys.*
414 *Res.* 76, 2213-2227.

415 Burke, M.L., W.L. Dimpfl, P.M. Sheaffer, P.F. Zittel, and L.S. Bernstein, 1996.
416 Formation of triplet CO in atomic oxygen flames of acetylene and carbon sub-oxide. *J.*
417 *Phys. Chem.* 100, 138-148.

418 Chan, W.F., G. Cooper, and C.E. Brion, 1993. The electronic spectrum of carbon dioxide.
419 Discrete and continuous photoabsorption oscillator strengths (6-203 eV). *Chem. Phys.*
420 178, 401-413.

421 Churyumov, K.I., G.F. Chorny, and V.V. Kleshchonok, 1997. Luminosity of the triplet
422 band of neutral CO molecules in the atmosphere of comet Scorichenko-George (1990
423 VI). *Astron. Astrophys. Trans.* 13, 225-231.

424 Churyumov, K.I., I.V. Luk'yanyk, et al., 2003. Spectral observations of comet C/2000
425 WM1 (linear) in Mexico. *Astron. Astrophys. Trans.* 22, 625-630.

426 Cochran, A.L. and W.D. Cochran, 2002. A high spectral resolution atlas of comet
427 122P/de Vico. *Icarus* 157, 297-308.

428 Conway, R.R., 1981. Spectroscopy of the Cameron bands in the Mars airglow. J.
429 Geophys. Res. 86, 4767-4776.

430 Cosmovici, C.B, C. Barbieri, C. Bonoli, F. Bortoletto, E. Hamzaoblu, 1982. On the
431 spectrum of comet Bradfield 1980t. Astron. Astrophys. 114, 373-387.

432 Fedorova, A.A., O.I. Korablev, J.-L. Bertaux, A.V. Rodin, F. Montmessin, D.A. Belyaev,
433 and A. Reberac, 2009. Solar infrared occultation observations by SPICAM experiment on
434 Mars-Express: Simultaneous measurements of the vertical distributions of H₂O, CO₂ and
435 aerosol. Icarus 200, 96-117.

436 Feldman, P.D., M.C. Festou, G.P. Tozzi, and H.A. Weaver, 1997. The CO₂/CO
437 abundance ratio in 1P/Halley and several other comets observed by IUE and HST.
438 Astrophys. J. 475, 829-834.

439 Fox, J.L. and A. Dalgarno, 1979. Ionization, luminosity, and heating of the upper
440 atmosphere of Mars. J. Geophys. Res. 84, 7315-7333.

441 Garcia-Muñoz, A., F.P. Mills, T.G. Slanger, G. Piccioni, and P. Drossart, 2009. The
442 visible and near-infrared nightglow of molecular oxygen in the atmosphere of Venus,
443 J. Geophys. Res. doi:10.1029/2009JE003447.

444 Gattinger, R.L., N.D. Lloyd, A.E. Bourassa, I.C. McDade, D.L. Degenstein, and E.J.
445 Llewellyn, 2009. Observation of the 557.7 nm to 297.2 nm brightness ratio in the auroral
446 spectrum with OSIRIS on Odin, Can. J. Phys. 87, 1133-1137.

447 Gattinger, R.L., A. Vallance Jones, D.A. Degenstein, and E.J. Llewellyn, 2010.
448 Quantitative spectroscopy of the aurora. VI. The auroral spectrum from 275 to 815 nm

449 observed by the OSIRIS spectrograph on board the Odin spacecraft, Can. J. Phys. 88,
450 559-567.

451 Gilijamse, J.J, S. Hoekstra, S.A. Meek, M. Metsälä, S.Y.T van de Meerakker, G. Meijer,
452 G.C. Groenenboom, 2007. The radiative lifetime of metastable CO($a^3\Pi$, $v = 0$), J. Chem.
453 Phys. 127, 221102.

454 Gudipati, M.S. and M. Kalb, 1998. New near infrared emission bands of CO: A highly
455 sensitive spectroscopic property of CO to probe the interstellar matter, Astron. Astrophys.
456 329, 375-379.

457 Huestis, D.L., 1994. DIATOM Spectral Simulation Program. Version 7 (SRI
458 International, Menlo Park, CA)

459 Huestis, D.L. S.W. Bougher, J.L. Fox, M. Galand, R.E. Johnson, J.I. Moses and J.C.
460 Pickering, 2008. Cross sections and reaction rates for comparative planetary aeronomy,
461 Space Science Reviews 139, 63-105, doi:10.1007/s11214-008-9383-7.

462 Johnson, J.R., U. Fink, and H.P. Larson, 1983. The 0.9-2.5 micron spectrum of Comet
463 West 1976 VI, Ap. J. 270, 769-777.

464 Judge, D.L. and L.C. Lee, 1973. Cross sections for the production of CO($a'-a$, $d-a$, $e-a$)
465 fluorescence through photodissociation of CO₂. J. Chem. Phys. 58, 104-107.

466 Krasnopolsky, V.A., A.A. Krysko, V.N. Rogachev, V.A. Parshev, 1976. Spectroscopy of
467 the Venus night airglow from the Venera 9 and 10 orbiters. Cosmic Res. 14, 789-795.

468 Krasnopolsky, V.A. and V.A. Parshev, V.A, 1983. Photochemistry of the Venus
469 atmosphere. In D.M. Hunten, L. Colin, T.M. Donahue, and V.I. Moroz, (Eds.), Venus.
470 The University of Arizona Press, Tucson, Arizona, pp. 431-458.

471 Krasnopolsky, V.A., 1983. Venus spectroscopy in the 3000-8000 Å region by Venera 9
472 and 10, Venus, 459-483. Eds. D.M. Hunten, M. Colin, T.M. Donahue, and V.I. Moroz,
473 University of Arizona Press, Tucson, AZ.

474 Krupenie, P.H., 1966. The band spectrum of carbon monoxide. NSRDS-NBS 5, U.S.
475 Dept. of Commerce.

476 Lawrence, G.M., 1972a. Photodissociation of CO₂ to produce CO(*a*³Π). J. Chem. Phys.
477 56, 3435-3442.

478 Lawrence, G.M., 1972b. Production of O(¹S) from photodissociation of CO₂. J. Chem.
479 Phys, 57, 5616-5617.

480 Leblanc, F., J.Y. Chaufray, J. Lilensten, O. Witasse, and J.-L. Bertaux, 2006. Martian
481 dayglow as seen by the SPICAM UV spectrograph on Mars Express. J. Geophys. Res.
482 111, E09S11.

483 Lee, L.C. and D.L. Judge, 1973. Population distribution of triplet vibrational levels of CO
484 produced by photodissociation of CO₂. Can. J. Phys. 51, 378-381.

485 Picazzio, E., A.A. de Almeida, S.M. Andrievskii, K.I. Churyumov, and I.V. Luk'yanyk,
486 2007. A high spectral resolution atlas and catalogue of emission lines of the Comet
487 C/2000 WM1 (LINEAR). Adv. Space Res. 39, 462-467.

488 Raghuram, S., and A. Bhardwaj, 2012. Model for the production of CO Cameron band
489 emission in Comet 1P/Halley. Planet. Space Sci. 63–64, 139-149.

490 Simon, C., O. Witasse, F. Leblanc, G. Gronoff, and J.-L. Bertaux, 2009. Dayglow on
491 Mars; Kinetic modeling with SPICAM UV limb data. Planet. Space Sci. 58, 1008-1021.

492 Slanger, T.G. and G. Black, 1970. The perturbation spectrum of CO. Chem. Phys. Lett. 4,
493 558-560.

494 Slanger, T.G. and G. Black, 1971. CO($a^3\Pi$), its production, detection, deactivation, and
495 radiative lifetime. J. Chem. Phys. 55, 2164-2173.

496 Slanger, T.G., P.C. Cosby, D.L. Huestis, and T.A. Bida, 2001. Discovery of the atomic
497 oxygen green line in the Venus night airglow. Science, 291, 463-465.

498 Slanger, T.G., P.C. Cosby, B.D. Sharpee, K.R. Minschwaner, and D.E. Siskind, 2006a.
499 O($^1S - ^1D, ^3P$) branching ratio as measured in the terrestrial nightglow. J. Geophys. Res.
500 111, A12318.

501 Slanger, T.G., D.L. Huestis, P.C. Cosby, N.J. Chanover, and T.A. Bida, 2006b. The
502 Venus nightglow: Ground-based observations and chemical mechanisms. Icarus, 182,
503 1-9.

504 Slanger, T.G., and J. L. Fox, 2009. The 557.7 nm oxygen green line in the Venus
505 nightglow. Bull. Amer. Astr. Soc. 41(3), 1127.

506 Slanger, T.G., B.D. Sharpee, D.A. Pejaković, D.L. Huestis, M. Bautista, R.L. Gattinger,
507 E.J. Llewellyn, I.C. McDade, D.E. Siskind, and K. Minschwaner, 2011. Calibration of
508 uv/visible instrumentation in orbit: observation and theory. Eos Trans. AGU. 92(35), 291.

509 Slanger, T.G., N.J. Chanover, B.D. Sharpee, and T.A. Bida, 2012. O/O₂ Emissions in the
510 Venus nightglow, Icarus (in press), doi:10.1016/j.icarus.2011.03.031.

511 Taylor, G.W. and D.W. Setser, 1971. Chemical applications of metastable argon atoms.
512 Generation, identification and characterization of CO($a^3\Pi$). Chem. Phys. Lett. 8, 51-54.

513 Tilford, S.G. and J.D. Simmons, 1972. Atlas of the observed absorption spectrum of
514 carbon monoxide between 1060 and 1900 Å. J. Phys. Chem. Ref. Data 1, 147-188, U.S.
515 Dept. of Commerce.

516 von Zahn, U., S. Kumar, H. Niemann, and R. Prinn, 1983. Composition of the Venus
517 atmosphere. In D.M. Hunten, L. Colin, T.M. Donahue, and V.I. Moroz, (Eds.), Venus.
518 The University of Arizona Press, Tucson, Arizona, pp. 299-430.

519 Wagner, R., F. Schouren, and M.S. Gudipati, 2000. Photochemically induced energy
520 transfer II: Spectroscopic and photophysical aspects of the electronic-to-electronic energy
521 transfer in geminate van der Waals complexes, J. Phys. Chem. A 104, 3593-3602.

522 Weaver, H.A., P.D. Feldman, J.B. McPhate, M.F. A'Hearn, C. Arpigny, and T.E. Smith,
523 1994. Detection of CO Cameron band emission in comet P/Hartley 2 (1991 XV) with the
524 Hubble Space Telescope. Astrophys. J. 422, 374-380.

525 Wysong, I. J., 2000. Measurement of quenching rates of CO($a^3\Pi$, $v = 0$) using laser
526 pump-and-probe technique, Chem. Phys. Lett. 329, 42-46.

527

528 **Figure Captions**

529

530 **Figure 1.** SPICAM Mars dayglow spectrum. Orbit 947; tangent ray height, 111 km;
531 latitude, 6 degrees N; SZA, 43 degrees (courtesy F. Leblanc).

532

533 **Figure 2.** DIATOM simulations of the CO Cameron bands in the region 190–240 nm for
534 $T = 500\text{--}10,000$ K, compared to SPICAM data (solid black line), resolution 1.6 nm.

535

536 **Figure 3.** ALS excitation spectrum for CO₂ photodissociation of a mixture containing
537 4 mTorr CO₂ in 2 Torr He. The combs show the vibrational level positions of the four CO
538 triplet states, with the arrows indicating the location of the $v = 0$ level.

539

540 **Figure 4.** Emission spectrum of CO triplet bands produced by CO₂ photodissociation of a
541 mixture containing ~6 mTorr CO₂ in 4 Torr He at 13.4 eV photon energy. The region
542 between 350 and 550 nm is not shown, as it only contains second order spectra of the
543 Cameron bands. The IR portion beyond 870 nm originates with the data of Burke et al.
544 [1996]. The spectrum has been corrected for variations in detector sensitivity as a
545 function of wavelength.

546

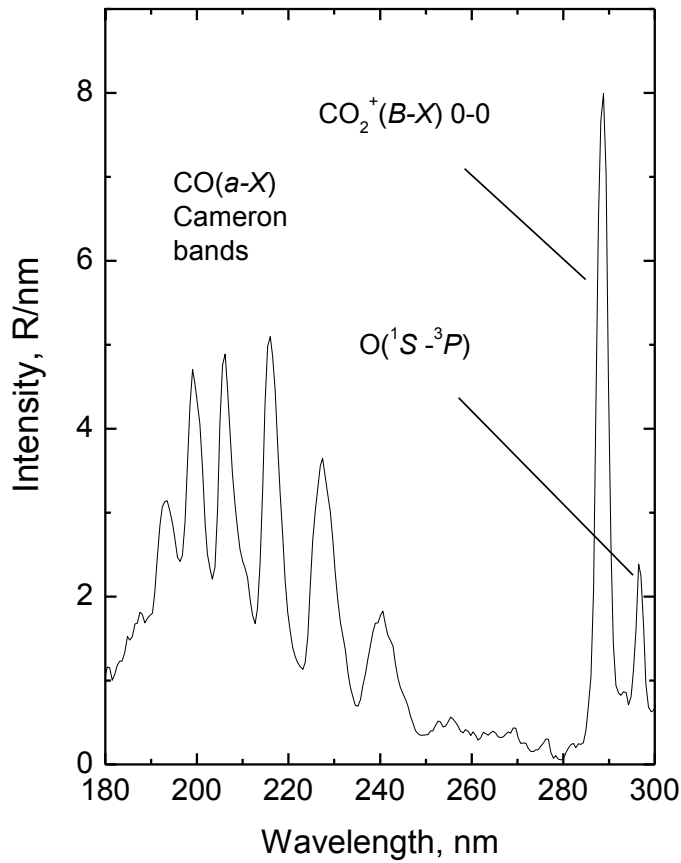
547 **Figure 5.** Unity optical depth for solar radiation as a function of photon energy in CO₂
548 atmospheres (Mars and Venus) for a vertical sun.

549

550

551

552 **Figures**

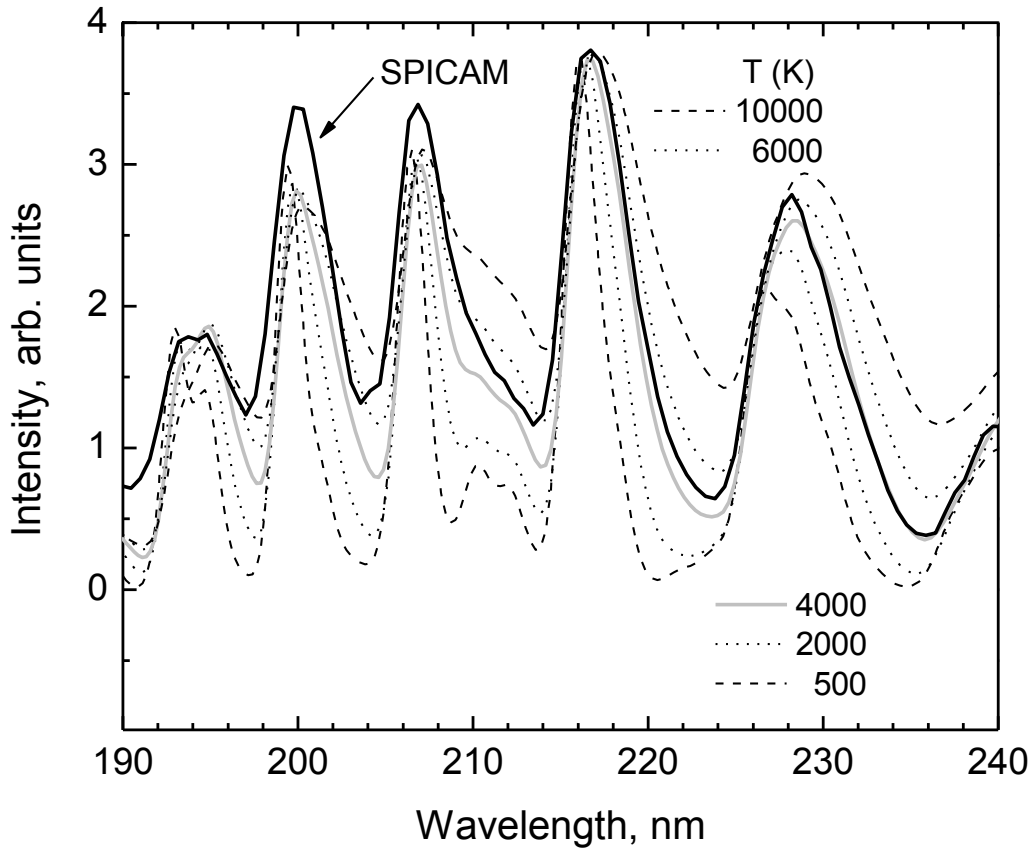


553

554 **Figure 1.** SPICAM Mars dayglow spectrum. Orbit 947; tangent ray height, 111 km;

555 latitude, 6 degrees N; SZA, 43 degrees (courtesy F. Leblanc).

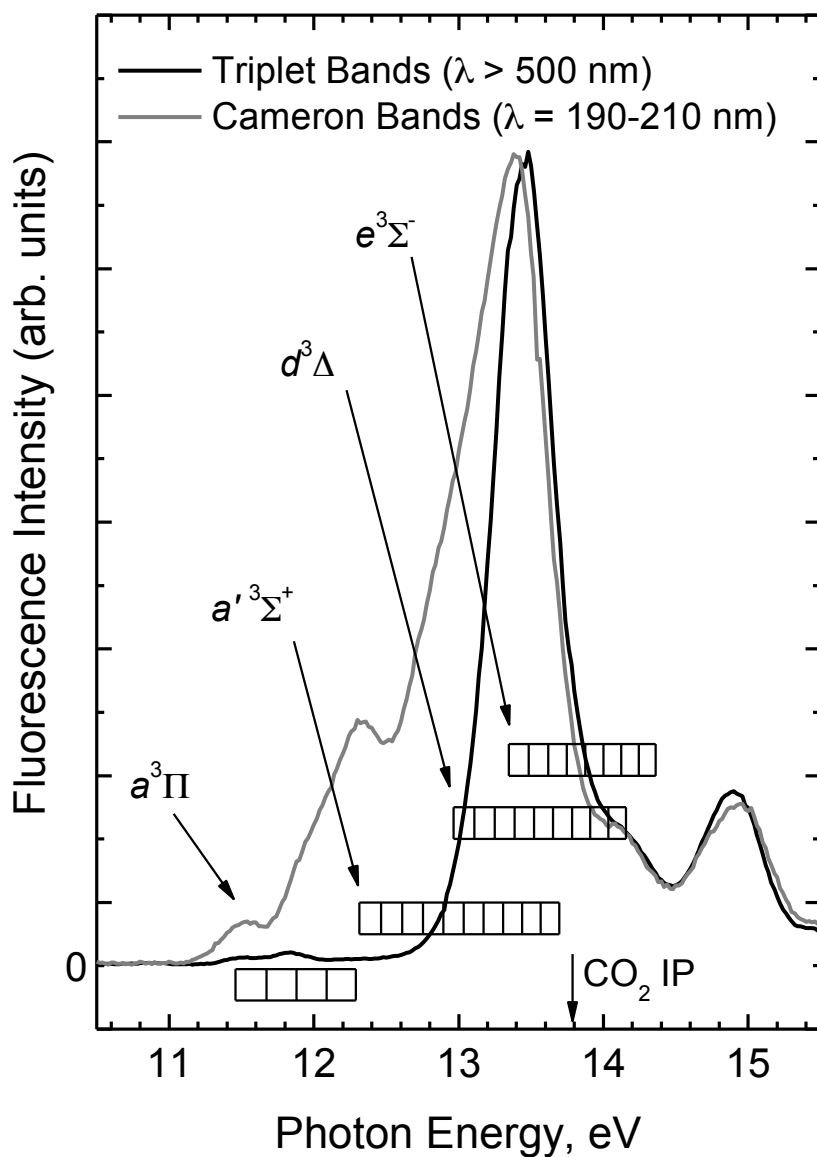
556



558
559

560

561 **Figure 2.** DIATOM simulations of the CO Cameron bands in the region 190–240 nm for
562 T = 500–10,000 K, compared to SPICAM data (solid black line), resolution 1.6 nm.

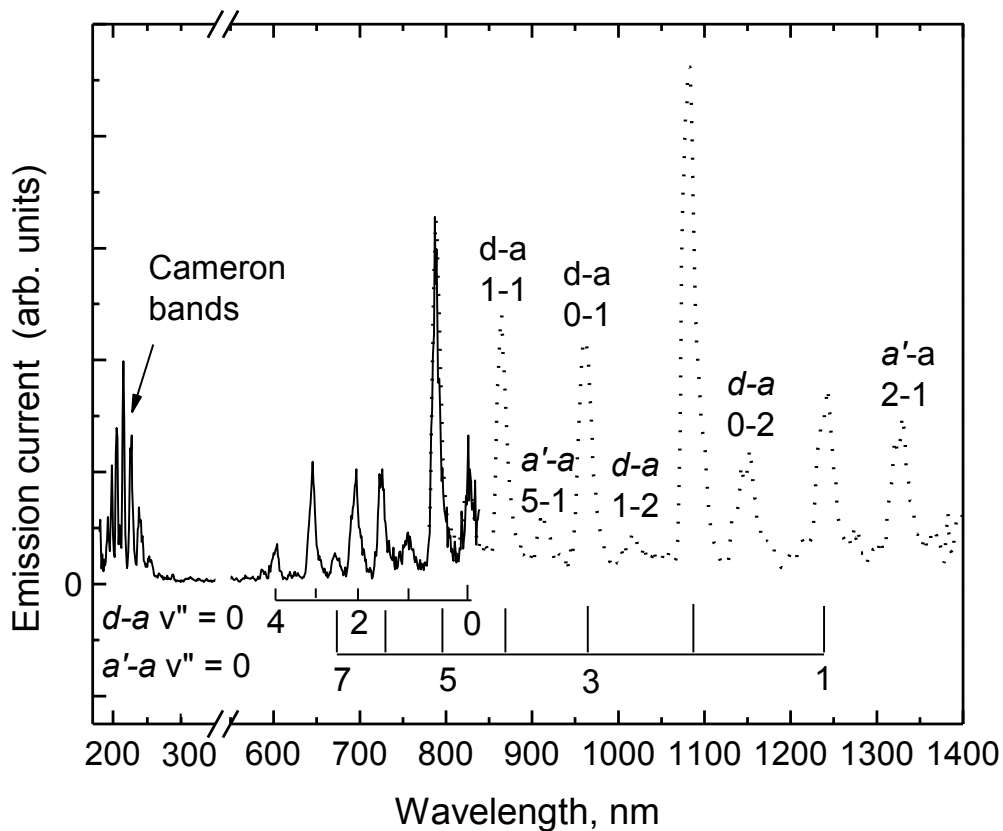


563

564

565 **Figure 3.** ALS excitation spectrum for CO₂ photodissociation of a mixture containing
 566 4 mTorr CO₂ in 2 Torr He. The combs show the vibrational level positions of the four CO
 567 triplet states, with the arrows indicating the location of the $v = 0$ level.

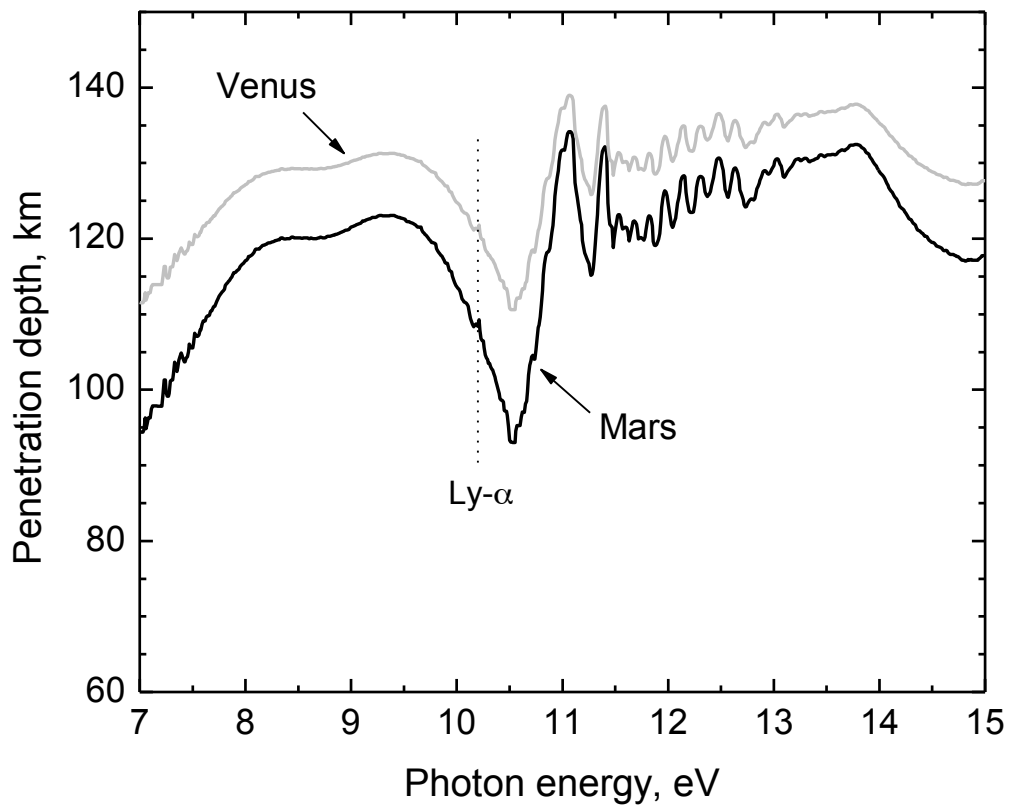
568



569

570

571 **Figure 4.** Emission spectrum of CO triplet bands produced by CO₂ photodissociation of a
 572 mixture containing ~6 mTorr CO₂ in 4 Torr He at 13.4 eV photon energy. The region
 573 between 350 and 550 nm is not shown, as it only contains second order spectra of the
 574 Cameron bands. The IR portion beyond 870 nm originates with the data of Burke et al.
 575 [1996]. The spectrum has been corrected for variations in detector sensitivity as a
 576 function of wavelength.
 577



578
579

580 **Figure 5.** Unity optical depth for solar radiation as a function of photon energy in CO₂
581 atmospheres (Mars and Venus) for a vertical sun.

582
583
584
585

This document was prepared as an account of work sponsored by the United States Government. While this document is believed to contain correct information, neither the United States Government nor any agency thereof, nor the Regents of the University of California, nor any of their employees, makes any warranty, express or implied, or assumes any legal responsibility for the accuracy, completeness, or usefulness of any information, apparatus, product, or process disclosed, or represents that its use would not infringe privately owned rights. Reference herein to any specific commercial product, process, or service by its trade name, trademark, manufacturer, or otherwise, does not necessarily constitute or imply its endorsement, recommendation, or favoring by the United States Government or any agency thereof, or the Regents of the University of California. The views and opinions of authors expressed herein do not necessarily state or reflect those of the United States Government or any agency thereof or the Regents of the University of California.